The fast response of volcano–seismic activity to intense precipitation: Triggering of primary volcanic activity by rainfall at Soufrière Hills Volcano, Montserrat

ADRIAN J. MATTHEWS,[a,b1] JENNI BARCLAY,[a] JADE E. JOHNSTONE[a]
[a]School of Environmental Sciences, University of East Anglia, Norwich, UK.
[b]School of Mathematics, University of East Anglia, Norwich, UK.

Journal of Volcanology and Geothermal Research (accepted)

May 27, 2009

[1] *Correspondence to:* Dr. Adrian Matthews, School of Environmental Sciences, University of East Anglia, Norwich, NR4 7TJ, UK. E-mail: a.j.matthews@uea.ac.uk. Tel: 01603 593733. Fax: 01603 591327.

ABSTRACT

One-minute resolution time series of rainfall and seismic data from the Soufrière Hills Volcano, Montserrat are analysed to explore the mechanism of external forcing of volcanic eruptions by rainfall over three years of activity. The real-time seismic amplitude (RSAM) shows a narrow, statistically significant, peak within 30 minutes after the start of intense rainfall events, and a much broader peak with a lag of 6–40 hours. The classified seismic events indicate that the volcanic response to rainfall begins at the surface and gradually penetrates deeper into the dome, as there is an increase in the pseudo-magnitude of: surface rockfall events (including pyroclastic flows) with lags from the first 30 minutes to 40 hours, long-period rockfalls (from shallow degassing) at lags of 4 and 14 hours, and long-period and hybrid events (source depth approximately 1 km) with lags at 14 and 24 hours after the start of rainfall events. There was no rainfall-related change in deeper, volcano–tectonic activity. There was no change in the frequency of any type of classified event, indicating that the rainfall acts to modulate existing, internal processes, rather than generating new events itself. These robust results are due to many (229) different rainfall events, and not just to a few, large magnitude cases. The rainfall-triggered volcanic activity examined here is consistent with a model of fast, shallow interactions with rainfall at the dome surface, after which, a deeper dome collapse follows.

Keywords: rainfall triggering; eruption; Montserrat; Soufrière Hills Volcano

1 Introduction

External triggering of volcanic activity has received much attention (e.g., Neuberg, 2000). Potential trigger mechanisms may involve atmospheric temperature, pressure and, more directly, precipitation or rainfall. The timing and extent of these external triggers are often predictable. Hence, in addition to the fundamental importance of how such mechanisms work, they can be of practical importance in volcanic hazard prediction and management. This study focuses on the triggering of volcanic activity by rainfall.

The external forcing of volcanic activity by rainfall has been recognised in a variety of differing settings, and can be responsible for a sudden escalation in hazardous eruptive behavior such as explosions and the major gravitational collapse of domes. This includes the triggering of eruptive episodes at basaltic volcanoes (Violette et al., 2001) including Strombolian explosions (Hort et al., 2003), shallow explosions at more silicic dome-forming eruptions (Mastin, 1994; Yamasato et al., 1998; Elsworth et al., 2004; Barclay et al., 2006) and lava dome collapse, meaning here a sustained volcanic event involving many individual rockfalls and pyroclastic flows over a period of up to a few hours (Yamasoto et al., 1998; Herd et al., 2005).

The timing of the volcanic response to rainfall can vary by several orders of magnitude. Anecdotal observations of this link typically relate renewed or reinvigorated volcanic activity and intense rainfall on the time scale of hours or days. All of these accounts detail the onset of volcanic activity within a few hours to a day or so of intense rainfall. However, the analysis of daily rainfall totals at several volcanoes demonstrate that correlations can also exist on the time scale of days. Mastin (1994) observed an increase in explosive tephra emissions at Mount St. Helens in the 2–15 day period following storms, and Yamasoto et al. (1998) found a similar relationship for both pyroclastic flows and dome collapse at Unzen, Japan.

The statistical analysis of a longer term data set of daily records from the Soufrière Hills Volcano (SHV), Montserrat (Barclay et al., 2006) demonstrated that the probability of observing a dome collapse on the SHV on any particular day increased by a factor of 6, to 9.3%, if more than 20 mm of rain fell on that day. Higher resolution data sets have recently become available, allowing the processes to be examined in much greater detail. Using minute-by-minute records of rainfall and seismic activity, Matthews et al. (2002) observed a volcano-seismic response just 2 hours after intense rainfall fell at the SHV during the dome collapse of 29 July 2001. Similarly, Hort et al. (2003) noticed an increase in the longevity of explosions at Stromboli volcano as recorded by Doppler radar in the hours following a single rainfall event. Neuberg (2000) found a correlation between seismicity, rainfall and ambient temperature on Mt. Batur and Merapi, Indonesia. Analysis on longer time scales with daily and seasonal fluctuations in rainfall has shown that rainfall can also modulate volcanic systems over several months at least (Violette et al., 2001; Mason et al., 2004).

1.1 Physical models

The observational studies in section 1 have led to the proposal of a wide variety of physical models to account for this activity. These models broadly involve one or more of: (a) the percolation of rainwater into the edifice and subsequent interaction with hot volcanic gases (Matthews and Barclay, 2004; Elsworth et al., 2004), (b) the mechanical erosion of talus by rainfall (Carn et al., 2004), (c) internal stresses associated with thermal contraction of the dome when cooled by rainfall (Mastin, 1994; Yamasoto et al., 1998), (d) the action of pressurised water or steam on potential failure surfaces within the dome (Simmons et al., 2004; Elsworth et al., 2004; Taron et al., 2007), (e) the long-term percolation of rainwater into the ground and its impact on the hydrological cycle (Violette et al., 2001). In all cases, the rainfall is assumed to be the final ingredient that triggers a volcanic system that is already primed for collapse. Typically, this may be during a period of

recent or ongoing dome growth, that has led to an over-steepened dome that is only marginally gravitationally stable. With the addition of a highly pressurised dome interior, the final addition of rainwater interacting with the dome by one or more of the mechanisms described above can be the final trigger for the system to release its instability. In an analagous manner, rainfall has also been attributed to triggering earthquake activity (Hainzl et al., 2006).

While there is strong evidence for a causal link between rainfall and increased volcanic activity, this can occur in many differing forms, from a minor increase in ash venting or volcanic tremor to major dome collapse involving the generation of lethal pyroclastic flows. To understand the hazard and improve monitoring and forecasting of these phenomena, it is also important to be aware of time intervals when this correlation weakens or changes. This paper represents the first attempt to analyse a high-resolution temporal link between rainfall and volcanic activity, and to relate it to these existing models. This approach allows us to assess the value of this type of data in predicting when and how heavy precipitation may impact an erupting volcano and where additional information about rainfall may be useful in forecasting volcanic eruptions. Fast interactions (minutes to a few hours) are associated with shallow activity but we also show that there is a correlation between rainfall and deeper perturbations to the system on longer time scales (many hours to days). We demonstrate that rainfall acts to modulate existing, internal processes rather than generating them itself. Further analysis of longer time-scale data sets now holds the promise of elucidating the likely conditions when this may give way to a major eruptive event.

1.2 Soufrière Hills Volcano

The SHV on the Caribbean island of Montserrat (16.7°N, 62.2°W; Fig. 1) has been active since July 1995. Its andesitic dome-forming eruption is one of the most well-monitored and highly instrumented eruptive episodes of recent times. Observations and inferences relating to its behaviour have also been extremely well documented (Druitt and Kokelaar, 2002). Since the observation of the first dome in November 1995 (Robertson et al., 1998) there have been four phases of dome growth to date: Phase I, November 1995–March 1998 (Calder et al., 2002), Phase II from November 1999–July 2003 (Herd et al., 2005), Phase III from August 2005–April 2007, and Phase IV from late 2008 onwards (http://www.mvo.ms). Each period of growth has had differing growth characteristics, with Phase I typified by relatively frequent, smaller collapses as well as periods of rapid dome growth and two series of repeated Vulcanian explosions (Druitt et al., 2002) and Phase II and III by rather less frequent but much larger dome collapses. Phase II had a rather slower average dome growth rate ($4\ m^3\ s^{-1}$; Herd et al., 2005) than Phase I but Phase III was characterised by some of the fastest periods of dome growth recorded to date (Loughlin et al., 2009). These periods of active dome growth have been separated by periods of repose (or residual periods). These have still involved some activity at the volcano including dome collapse and shallow explosions (Norton et al. 2002).

The analysis in this paper largely deals with Phase II of the dome growth and part of the following period of repose, using rainfall and seismic data recorded between 1 January 2001 and 31 December 2003. The second phase of growth terminated after the largest dome collapse that has occurred at the SHV to date on 13 July 2003 (Herd et al., 2005).

The data and methodology are described in section 2, and section 3 then describes the observed volcano–seismic response to rainfall. The sensitivity to the details of the methodology is presented in 4, and the discussion and conclusions in 5.

2 Data and methodology

2.1 Rainfall and RSAM data

A network of 8 one-minute resolution tipping-bucket rain gauges was deployed around the volcano (Fig. 1), from January 2001 onwards. Real-time seismic amplitude (RSAM; Endo and Murray, 1991) time series data were used as a proxy for volcanic activity. The RSAM data are a measure of the overall seismic energy, integrated over all frequency bands. Data at one-minute resolution from 1 January 2001 to 31 December 2003 were used, from 3 short-period seismometers and 3 broadband seismometers (Fig. 1).

A binary rainfall "event" time series was created from the raw data, also with a temporal resolution of 1 minute. A value of "1" indicates the start of a rainfall event, with a value of "0" otherwise. Both intensity and total amount of rainfall are likely to be important in triggering volcanic activity (Matthews and Barclay, 2004). Hence, a threshold rainfall rate of 5 mm of rain falling in 60 minutes was defined. The binary rainfall event time series was created by stepping in time through the rainfall data. When the threshold was exceeded by *any* of the operational gauges, a rain event (a "1") was defined at the start of that 60-minute period. A repose time of 24 hours must then pass, with no rainfall recorded at any gauge, before the next rainfall event can be defined. This repose time prevents a single meteorological rainfall system being recorded as multiple rainfall events.

For example, in the case study of 22 October 2002 (Fig. 2a) a rainfall event was defined at 1521 UTC. Enhanced seismic activity (high RSAM) can clearly be seen 2–4 hours after the start of the rainfall event, associated with pyroclastic flows down Tuitt's Ghaut and the Tar River valley. Similarly, a rainfall event was defined at 1013 UTC on 12 July 2003 (Fig. 2b). This was followed within 30 minutes by a gentle ramping up of seismic activity over the next 15 hours, and then a rapid increase in seismic activity, associated with one of the largest dome collapses on record, with a collapse volume of 210×10^6 m^3 (Herd et al., 2005). This collapse was preceded by considerable seismic activity over the previous few days, and the intense rainfall may have provided the final trigger.

During the 3-year period from 1 January 2001 to 31 December 2003, 229 such rainfall events were identified, using the standard parameters described above. Individual events are likely to contain extra signals that are independent of any rainfall-triggered processes. Hence, the remaining analysis is carried out using composite means, averaged over all 229 events.

The time of the i'th rainfall event is denoted as t_i. Rainfall is expected to impact the volcanic activity at SHV on short time scales, of the order of hours or days. Hence, high-pass filtered RSAM anomaly time series $R'(t)$ were constructed by subtracting the 10-day running mean from the original RSAM time series. This removed the low-frequency variability and instrument drift. To determine the mean seismic response to rainfall, the composite RSAM activity $\overline{R}$ at lag k was calculated by summing the RSAM anomalies over a $\Delta t = 30$ minute bin, lagged by $k\,\Delta t$ relative to each of the n rainfall events,

$$\overline{R}_k = \frac{1}{n} \sum_{i=1}^{n} \left[\sum_{t=t_i+k\,\Delta t}^{t_i+(k+1)\,\Delta t} R'(t) \right]$$

For example, a lag of $k = 3$ corresponds to the seismic activity between 90 and 120 minutes after the start of the rainfall event. Negative values of k correspond to negative lags (seismic activity preceding the start of the rainfall event).

As an example, the lagged composite RSAM for the Garibaldi Hill seismometer (Fig. 3a) shows a background level of about 150 RSAM units with some isolated, narrow peaks above this at negative lags, i.e., seismic activity preceding the rainfall events at zero lag. There is a broad peak at positive

lags, with enhanced seismic activity between the first 30 minutes and 40 hours after the start of the rainfall events. At higher lags, the seismic activity returns to its background level. A 7-point running mean (thick line in Fig. 3a) is used to smooth over the noise.

Due to the high temporal autocorrelations in the rainfall and seismic time series, calculation of the statistical significance of the peaks needed to be addressed carefully. A Monte Carlo approach was used. Synthetic rainfall time series were created by randomly reordering 5-day periods within the wet (July–December) and dry (January–June) halves of each year from the original rainfall time series. This approach was chosen to preserve the autocorrelation properties of the original rainfall time series. Lagged RSAM composites were calculated from each of 10,000 such randomised rainfall time series. A null distribution of the 7-point filtered RSAM anomaly was then calculated. As an example, the 95th percentile of this distribution for the Garibaldi Hill seismometer was found to be 284 RSAM units, shown by the thick horizontal line indicating the 95% "local" significance level in Fig. 3a. Hence, the broad peak at positive lags is significant at the 95% level for lags between approximately 4 and 40 hours. Furthermore, the "global" significance (Livezey and Chen, 1983) was also assessed from another null distribution, of the numbers of individual lag bins that passed the local significance test. The number of bins in the Garibaldi Hill composite (Fig. 3a) that were locally significant exceeded the 95th percentile of this null distribution, hence the composite as a whole is globally significant.

The composite analysis of RSAM anomaly described above may be biased by a small number of very large-amplitude seismic perturbations occurring shortly after rainfall events. To test the robustness of the rainfall–seismic relationship, an alternative approach was used. Instead of using the *amplitude* of the seismic signal, the *number* of events above a certain seismic threshold were composited. First, 5-minute averages were calculated from the 1-minute resolution RSAM and rainfall time series. A seismic event binary time series was then created, with a "1" if a seismic threshold of 500 counts min^{-1} was exceeded for a particular 5-minute interval, and a "0" otherwise. A lagged composite of the number of seismic events was then created in a similar manner to the seismic amplitude composites of Fig. 3. The lags were calculated in 30-minute bins, as before. Hence, the maximum that any particular seismic event could contribute to a given lag bin would be "6", when the seismic threshold was exceeded in all six of the 5-minute bins in that 30-minute window. The results from these composites of the number of seismic events (Fig. 4) are very similar to those from the RSAM composites (Fig. 3).

2.2 Classified event data

The RSAM composites are used to describe the gross response of the volcano to intense rainfall. Now, information from individual seismic events is analysed to infer the likely mechanisms by which the volcano responds to rainfall. As part of the MVO monitoring program, seismic events were operationally defined from manual inspection of the real-time seismic waveforms. Each seismic event was manually classified as either a rockfall, long-period rockfall, long-period, hybrid, or volcano–tectonic event, based on the shape, frequency content, and duration of the waveform (Miller et al., 1998; Neuberg et al., 1998; de Angelis et al., 2007).

The types of classified events are discussed briefly here, in nominal order of increasing depth within the dome. Rockfalls have two seismic sources. Rockfall events are generally in the 2–8 Hz range, and are generated by falling debris on the surface of the dome. Pyroclastic flow signals lack clear seismic phases, are longer duration than rockfall signals but have similar broadband waveforms (1–20 Hz range). The "rockfall" event classification adopted by the MVO includes both surface rockfalls and pyroclastic flows. The additional occurrence of a second marked spectral peak in the 1–2 Hz range has lead to the classification of "long-period rockfall" events (Luckett et al., 2002; Calder et al., 2005). These originate slightly below the surface, and are attributed to shallow

degassing processes.

Long-period and hybrid events have a similar physical origin and can be considered as end members of a spectrum of behaviour (Neuberg et al., 2000), related to brittle failure of magma at the glass transition in the upper conduit and dome (Neuberg et al., 2006). The long-period and hybrid events both have low-frequency coda caused by fluid-filled conduit resonance; hybrids are additionally triggered by a precursory signal from fracture/shear slip. These events occur at a relatively shallow depth within the dome or upper conduit; hypocentres for swarms of these "low-frequency" (0.2–5 Hz) earthquakes in 1997 were inferred to cluster directly under the lava dome at depths as shallow as 1 km (Baptie et al., 2002) or between 1.3 and 1.6 km between 1995 and 1996 (Rowe et al., 2004). Models of the pressure source of associated tilt cycles also suggest that this should occur at depths of less than 1 km (Green et al., 2006) and a recent model allows for the development of shear banding at depths less than 700 m (Hale and Mühlhaus, 2007).

Higher frequency volcano–tectonic events are associated with brittle rock failure and exhibit shear-fault source mechanisms consistent with a location lower in the crust around the conduit (Roman et al., 2006).

Composites of the *number* of each type of event, lagged in 30-minute bins with respect to the start of the rainfall events, were calculated (not shown). There were no significant peaks. Hence, intense rainfall does not significantly modulate the number, or frequency of occurrence, of the different types of classified event. However, there may be a systematic underestimation of the number of events immediately following rainfall-triggered volcanic activity as, in some cases, the whole seismic network failed for several hours after the start of large-magnitude events such as dome collapse. Also, smaller amplitude rockfall signals could be masked by larger amplitude pyroclastic flows.

Where possible, a pseudo-magnitude was also provided for each classified event (Jaquet et al., 2006). This was not possible if much of the seismic network was out of operation (during and because of a large event), or if the event was only recorded on the analogue seismometers, which were uncalibrated. Pseudo-magnitude M is proportional to the logarithm of energy E, $M = a + b \log E$, where the constants a and b were fitted using data from several regional earthquakes recorded at the Windy Hill short-period seismometer, which had very low noise levels. The location of each seismic event was unknown and assumed to be at sea level, directly below the dome. Hence the magnitudes are pseudo-magnitudes, rather than absolute magnitudes. Nevertheless, with these caveats they are a quantitative measure of the energy released in each classified event. Similar to the RSAM composites, lagged composites of the pseudo-magnitude of each type of classified event were then calculated (Fig. 5).

3 The volcano-seismic response to rainfall

The volcano-seismic response to intense rainfall on the SHV is now discussed, using information from the lagged composites of RSAM anomalies (Fig. 3) and number of events (Fig. 4) at each seismometer, and the pseudo-magnitude of each type of classified event (Fig. 5).

There are no statistically significant peaks in the 7-point running mean RSAM amplitude at negative lags at any station (Fig. 3). Strictly speaking, the 7-point mean RSAM anomalies are statistically significant at slightly negative lags (-1 to 0 hours) at Long Ground and Roche's Yard (Fig. 3d,f), but these are clearly a leakage from the peak at $+0.25$ hours due to the 7-point running mean process. There is just one significant peak at negative lags in all the composites of the number of seismic events (at a lag of -15 hours at St. George's Hill; Fig. 4b). There are minor significant peaks at negative lags in some of the classified event composites (Fig. 5), but no more than would be expected by chance, as the local significance level was set at 95%. Formally, none of the lagged composites in Figs. 3, 4 and 5 are globally significant when tested over the -72 to 0 hour negative

lag range. Hence, as expected, seismic activity does not precede rainfall. This is in stark contrast to the clearly elevated and significant measures of seismic activity that follow rainfall, at positive lags.

Immediately following the start of the rainfall events, all seismometers show a distinct, narrow peak in the 0–30 minute lag bin (Figs. 3, 4). It is particularly pronounced at the Long Ground and Roche's Yard stations, which are situated either side of the Tar River Valley, the main channel for pyroclastic flow activity during Phase II. The peak is also very strong at the St. George's Hill seismometer, which also lies near a drainage channel, the Belham valley. The inference from this is that these events are mainly associated with seismic energy generated from surface activity. The 7-point running mean composites (thick line in Figs. 3, 4) at these three stations are statistically significant at the 95% level at this 0–30 minute lag. The peak is still present at the other three stations (Garibaldi Hill, Windy Hill, South Soufrière Hills), and also in the rockfall classified events (Fig. 5a), but is relatively weaker compared to peaks at later lags. As the peak is very narrow (typically in just one or two lag bins), it is not statistically significant in the 7-point running mean composites.

The distinct 0–30 minute peak is the start of a much broader peak in seismic activity, between approximately 1 and 20 hours lag, at the Garibaldi Hill and St. George's Hill stations. This is to be likely due to the passage of rainfall-triggered lahars in the neighbouring Belham Valley. This broad peak is also evident in the rockfall classified events (Fig. 5a). The long-period rockfall events show a distinct, statistically significant peak at a lag of 4 hours (Fig. 5b).

Closer to the volcano, the Roche's Yard station also exhibits a broad peak in the 1–20 hour lag range, but with a clear peak in RSAM amplitude near 12 hour lag (Fig. 3e). The Windy Hill and South Soufrière Hills stations display rather narrower peaks in RSAM amplitude at approximately 12–20 hours after the onset of rainfall. This coincides with statistically significant peaks in the long-period rockfall (12–16 hours; Fig. 5b) and long-period (12–16 hours; Fig. 5c) classified events, and a just-significant peak in hybrid events (14–16 hours; Fig. 5d). Hence, this 12–16 hour peak is indicative of a signal generated deeper within the dome. Note that the maximum distance of any seismometer from the volcano is only 6 km. Hence, the travel times for seismic waves are negligible, on the order of a second, while the data are then analysed into 30-minute bins.

There then appears to be a lull in seismic activity, with a minimum in RSAM amplitude (Fig. 3), at all stations at a lag of 22 hours after the start of the rainfall events.

Activity then increases again, with clear maxima in both RSAM amplitude and number of events in the lag range 24–32 hours. This peak is statistically significant at all stations except Windy Hill (where the earlier 12–16 hour peak is so pronounced that it has lead to a very high threshold significance level for that station). Correspondingly, there is a significant peak in the hybrid classified events (Fig. 5d) at a 24-hour lag. This coincides with an increase in the number of surface rockfall events (Fig. 5a) at a lag of 24 hours, which then continues at a weaker level up to a lag of 39 hours. Hence, there appears to be a secondary episode of deeper activity (hybrids) 24 hours after the start of rainfall events, which then triggers further surface activity the following day, consistent with the analysis of daily records by Barclay et al. (2006). All the RSAM composites in Fig. 3, and the rockfall, long-period rockfall, long-period and hybrid composites (Fig. 5a–d) are globally significant, when tested over the full -72 to 72 hour lag range, and just the positive lag range (0 to 72 hours).

Volcano–tectonic events are associated with brittle failure at depth, from stress changes associated with magma transport and storage. Not surprisingly, these show no relationship with intense rainfall. There are no significant peaks in the lagged composite (Fig. 5e), which is not globally significant.

4 Sensitivity to methodology

The lagged composite of the number of seismic events for a range of seismic thresholds (100–1000 counts min^{-1}) at Roche's Yard (Fig. 6) shows that the methodology is not sensitive to the exact threshold used. As the seismic threshold is increased, the number of seismic events decreases for any given lag, as expected. However, the positions (lags) of the main peaks do not change with seismic threshold. Note that the composite for Roche's Yard in Fig. 4e is a cross section, at 500 counts min^{-1}, through the diagram in Fig. 6.

The methodology is also tested for sensitivity to the repose period. For example, the lagged composite of the number of seismic events at South Soufrière Hills with a repose period of just 1 hour (Fig. 7) can be compared against the composite with the standard repose period of 24 hours (Fig. 4f). The results are not qualitatively changed. The narrow peak at the 0–30-minute lag bin and the broad peak in the 6–40-hour lag range are still present. As expected, the number of events recorded shows an overall increase, as the shorter repose period allows longer-lived rainfall events to contribute more than once to the composite, and at different lags. Because of this, the sharp peaks tend to become smeared out and do not stand above the background so clearly. The sensitivity to these parameters was comprehensively tested for all seismometers (not shown), and the qualitative results were not changed. Similarly, the results were not qualitatively sensitive to the rainfall threshold used.

To extract further information on the volcano-seismic response to rainfall, a Fourier transform of the waveform for each individual seismic event was routinely calculated at the MVO. The power spectrum was then averaged over 11 frequency bands: 0.1–1, 1–2, 2–3, 3–4, 4–5, 5–6, 6–7, 7–8, 8–9, 9–10 and 10–30 Hz. The power in each frequency band was expressed as a percentage of the total power, summed over all 11 frequency bands, for that particular seismic event. Here, composites of the percentage of energy in each frequency band, lagged with respect to the start of the rainfall events, were calculated. Surface seismic activity, due to the rockfalls and pyroclastic flows that are triggered by intense rainfall, has a predominantly high-frequency component (Neuberg et al., 1998; de Angelis et al., 2007). Consistent with this model, the composite for the highest frequency band (10–30 Hz; Fig. 8) does show peaks in seismic activity, at 45 minutes and 26 hours after the start of the rainfall events. The 9–10 Hz band also has a peak at 26 hours, while none of the other frequency bands have any significant peaks.

5 Discussion and conclusions

In a composite study of 229 individual rainfall events, significant peaks in volcano–seismic activity following intense rainfall have been observed at Soufrière Hills Volcano, Montserrat, during phase II of the on-going eruption. These are summarised in a schematic diagram (Fig. 9), and discussed with reference to the original figures. Immediately after intense rainfall starts, there is an elevation in the composite RSAM signal at all seismometers around the volcano (Fig. 3). Analysis of classified data reveals that this is due to an increase in the pseudo-magnitude of the surface rockfall/pyroclastic flow classified events (Fig. 5a). After the initial, sharp peak within the first 30 minutes of the start of rainfall events, the RSAM activity and rockfall classified events remain at elevated levels for a further 16 hours.

However, during this time the seismic response to rainfall shifts from the surface to deeper within the volcano. A distinct peak at 4 hours lag after the start of the rainfall events is observed in the long-period rockfalls. These events are attributed to shallow degassing that triggers surface rockfalls (Luckett et al., 2002). At 14 hours after the start of the rainfall events, the pseudo-magnitude of long-period rockfall (Fig. 5b), long-period (Fig. 5c) and hybrid (Fig. 5d) classified events also peak.

A distinct lull in activity follows, at a lag of 22 hours after the start of the rainfall events. Subsurface activity then continues, demonstrated by peaks in the pseudo-magnitude of hybrid events at a lag of 24 hours. The increased pseudo-magnitude of rockfall events and RSAM accompanies this behavior, and then continues on to a lag of approximately 40 hours.

Hence, the initial response of the volcano to rainfall takes the form of rockfalls and pyroclastic flows, which attests to the removal of surface material. This is followed within four hours by significant peaks in behaviour associated with shallow degassing and (long-period) rockfalls. This indicates that shallow mechanical interactions are now replaced by a deeper perturbation within the dome itself, as water penetrates the interior and is heated (Elsworth et al., 2004), or as the upper layers are removed by rockfalls and pyroclastic flows. At time intervals longer than four hours, a threshold appears to be reached as distinct peaks in rockfall/pyroclastic flow activity are observed at lags of 14 and 24 hours (Fig. 5a). This seems to suggest that the more deep-seated response in an unstable dome can trigger dome collapse, or at least further instability at the surface. For example, the dome collapse of 14 October 2001 was initiated 5.5 hours after the onset of intense rainfall, peaking at approximately 11 hours lag, and the very large collapse of 12–13 July 2003 (Herd et al., 2005) intensified around 12–14 hours after a period of intense rainfall. This later rockfall/pyroclastic flow activity lasts for up to 40 hours after the start of the rainfall event, at which point seismic activity returns to its background levels. The timing of these events are consistent with, but on a much higher temporal resolution than, the analysis of daily mean data from the Soufrière Hills Volcano in Barclay et al. (2006).

These results are robust to the details of the methodology employed, as discussed in the sensitivity tests (section 4). An intriguing null result is that only the (pseudo) *magnitudes* of the classified rockfall, long-period rockfall, long-period, and hybrid events are significantly affected by rainfall. There is no significant modulation of the *number* of these classified events. This implies that the rainfall acts to modulate volcanic processes that would have happened anyway. The classified events (rockfall, long-period rockfall, long-period, and hybrid) occur as part of an internally-driven, volcanic system. When the surface forcing from an intense rainfall event is added to this system, it appears to amplify the internally-driven processes. If the dome is already in a state that is primed to collapse, this extra perturbation from the rainfall-amplified volcano-seismic activity destabilises the system, and can lead to the catastrophic dome collapses that are observed to occur within 1–2 days of intense rainfall (Barclay et al., 2006), with some of the larger, documented dome collapses occuring within a few hours (Matthews et al., 2002).

It is worth noting that a potentially complicating factor, that of a diurnal cycle in the timing of rainfall events, was not important here. The start times of the rainfall events were, perhaps surprisingly, randomly scattered throughout the day. There were also no lagged autocorrelations in rainfall, with a monotonic decrease in rainfall following the start of the rainfall events, at lag zero. The analysis methodology also included a repose time, of 24 hours of zero rainfall at any rain gauge, that must pass before the next rainfall event could be defined. Hence the rainfall events can be considered as independent, impulsive perturbations to the volcanic system, greatly simplifying the interpretation.

Theoretical models of the mechanisms of rainfall-triggered dome collapse need to take account of the temporal behaviour observed in this study. In particular, they should simulate an almost immediate increase in surface activity, together with an approximate time scale of 12–24 hours to trigger a deep-seated collapse. The cessation of activity approximately 40 hours after initiation represents an upper limit on the response time scale.

The thermodynamic energy flux model of Matthews and Barclay (2004) predicts that the dome surface temperature will cool very rapidly (from several hundred to 100 °C, the boiling point of water) within minutes of rainfall onset, due to the latent heat flux from evaporation of rain water. This could then allow the quench fragmentation mechanism (Mastin 1994; Yamasoto et al., 1998)

to act, triggering rockfalls and pyroclastic flows. The dome can also be modelled as a permeable matrix with an upward flux of magmatic gas supplied from depth (Hicks et al., 2009a). Rain water can infiltrate into the matrix, partially blocking this gas flow. The resulting rapid increase in interior pore pressure can be sufficient to cause failure of the upper layers within minutes (Hicks et al., 2009b), again triggering rockfalls and pyroclastic flows. Once a surface layer of rock has been removed, the resulting gas pressure perturbation rapidly propagates downwards, communicating the surface signal to the deeper interior in a time scale of a few minutes (Hicks et al., 2009a). All of these processes would occur within the first 30 minutes after the start of the rainfall events, i.e., within the first lag bin of the composite analyses, and could contribute to the peak there.

The later peaks (up to 40 hours after the start of the rainfall events) and downward migration of the volcanic response are not explained by these surface models. Two possible scenarios emerge: 1) Once the surface layers have been removed by direct interaction with rainfall, internal processes within the unstable dome take over, that are not dependent on penetration of rainwater deep into the interior; 2) alternatively, rain water may infiltrate deep into the dome, possibly causing failure along pre-existing internal surfaces (Elsworth et al., 2004; Taron et al., 2007). Talus erosion can also not be ruled out, but if it were the only mechanism in operation we would not perhaps expect the distinct peaks, but rather a broad, diffuse peak.

The triggering of volcanic activity at the SHV by rainfall is of clear importance for volcanic hazard prediction and mitigation. Of equal interest here are the periods when rainfall may *not* have a significant influence on the volcano. During the study period 2001–2003, rainfall has been shown to modulate the amplitude of volcano-seismic processes, but not their frequency. The implication is that for deep-seated interactions the volcano must be in a state where hybrid, long period and long-period rockfalls are likely to be generated. Rockfall frequences on Montserrat have already shown a statistical link to extrusion rate that breaks down at low extrusion rates (Calder et al., 2005). It is also likely that the system response to rainfall will vary with the geometry of the dome: e.g., immediately after a collapse or during periods of repose. Hence, the time since the last threshold failure could be another important parameter in the system (Taron et al., 2007). Our preliminary analysis has demonstrated the value of high-resolution data sets in elucidating the underlying processes behind volcano–rainfall interactions. As longer time series of data become available to us, we will be able to sub-divide this data set into periods with high and low extrusion rates, repose intervals and those periods associated with active internal dynamics. All of these should allow discrimination between dome states where rainfall-induced activity is particularly likely and when it is not, and which mechanisms preside over each type of interaction.

Furthermore, the analysis carried out here only considered the response of the volcano within ± 10 days of the start of individual rainfall events. Results were only presented for lags between -3 and 3 days, as there were no volcano-seismic signals outside this lag range. A preliminary separation of the 2001–2003 data into wet (July–December) and dry (January–June) showed that the correlation between volcanic activity and rainfall was only pronounced during the wet season. However, this finding was not statistically significant due to the subdivision of our shorter time period. This does demonstrate the clear potential of investigating much slower interactions on the time scale of months, as found by Violette et al. (2001) at the Piton de la Fournaise Volcano, Reunion.

In summary: using data from multiple (> 200) events, we have shown a robust and statistically significant volcano-seismic response to intense rainfall during Phase II of the ongoing eruption at the Soufrière Hills Volcano, Montserrat. The temporal sequence of events suggests a volcano–rainfall interaction at the surface that begins within minutes of the start of intense rainfall events. This interaction then spreads downwards into the dome on a time scale of hours to approximately two days, and may culminate in dome collapse and explosive behaviour. These results will be of relevance to volcanic hazard prediction and mitigation, as well as to fundamental studies of dome collapse

and explosive activity.

ACKNOWLEDGEMENTS

We thank the past and present staff of the Montserrat Volcano Observatory for the RSAM, classified event and spectral data, maintenance of rain gauges, and hospitality during field visits. We thank Richard Herd, Peter Hicks and Mark Cooker for helpful discussions, and Richard Herd, Eliza Calder, Derek Elsworth and an anonymous reviewer for comments that helped to improve the manuscript. JEJ's studentship was funded by the School of Environmental Sciences, University of East Anglia.

REFERENCES

Baptie, B., Luckett, R., Neuberg, J., 2002. Observations of low-frequency earthquakes and volcanic tremor at Soufrière Hills Volcano, Montserrat. In Druitt, T.H., Kokelaar, B.P., (eds), 2002: The eruption of Soufrière Hills Volcano, Montserrat, from 1995 to 1999. Geological Society, London, Memoirs. 611–620.

Barclay, J., Johnstone, J. E., Matthews, A. J., 2006. Meteorological monitoring of an active volcano: Implications for eruption prediction. J. Volcanol. Geotherm. Res. 150, 339–358.

Calder, E. S., Luckett, R., Sparks, R. S. J., Voight, B., 2002. Mechanisms of lava dome instability and generation of rockfalls and pyroclastic flows at Soufrière Hills Volcano, Montserrat. In Druitt, T.H., Kokelaar, B.P., (eds), 2002: The eruption of Soufrière Hills Volcano, Montserrat, from 1995 to 1999. Geological Society, London, Memoirs. 173–190.

Calder, E. S., Cortes, J. A., Palma, J. L., Luckett, R., 2005. Probabilistic analysis of rockfall frequencies during an andesite lava dome eruption: The Soufrière Hills Volcano, Montserrat. Geophys. Res. Lett. 32, L16309. doi: 10.1029/2005GL023594.

Carn, S. A., Watts, R. B., Thompson, G., Norton, G. E., 2004. Anatomy of a lava dome collapse: The 20 March 2000 event at Soufrière Hills Volcano, Montserrat. J. Volcanol. Geotherm. Res. 131, 241–264.

de Angelis, S., Bass, V., Hards, V., Ryan, G., 2007. Seismic characterization of pyroclastic flow activity at Soufrière Hills Volcano, Montserrat, 8 January 2007. Nat. Hazards Earth Syst. Sci. 7, 467–472.

Druitt, T. H., Young, S. R., Baptie, B., Bonadonna, C., Calder, E. S., Clarke, A. B., Cole, P. D., Harford, C. L., Herd, R. A., Luckett, R., Ryan, G., Voight, B., 2002. Episodes of cyclic Vulcanian explosive activity with fountain collapse at Soufrière Hills Volcano, Montserrat. In Druitt, T.H., Kokelaar, B.P., (eds), 2002: The eruption of Soufrière Hills Volcano, Montserrat, from 1995 to 1999. Geological Society, London, Memoirs. 281–307.

Druitt, T. H., Kokelaar, B. P., 2002. The eruption of Soufrière Hills Volcano, Montserrat, from 1995 to 1999. Geological Society, London.

Elsworth, D., Voight, B., Thompson, G., Young, S. R., 2004. Thermal-hydrologic mechanism for rainfall-triggered collapse of lava domes. Geology 32, 969–972.

Endo, E. T., Murray, T. L., 1991. Real-time seismic amplitude measurement (RSAM): A volcano monitoring and prediction tool. Bull. Volcanol. 53, 533–545.

Green, D. N., Neuberg, J., Cayol, V., 2006. Shear stress along the conduit wall as a plausible source of tilt at Soufrière Hills volcano, Montserrat. Geophys. Res. Lett. 33, L10306. doi: 10.1029/2006GL025890.

Hainzl, S., Kraft, T., Wassermann, J., Igel, H., Schmedes, E., 2006. Evidence for rainfall-triggered earthquake activity. Geophys. Res. Lett. 33, L19303. doi: 10.1029/2006GL027642.

Hale, A. J., Mühlhaus, H. B., 2007. Modelling shear bands in a volcanic conduit: Implications for over-pressures and extrusion rates. Earth Planet. Sci. Lett. 263, 74–87.

Herd, R. A., Edmonds, M., Bass, V. A., 2005. Catastrophic lava dome failure at Soufrière Hills Volcano, Montserrat, 12–13 July 2003. J. Volcanol. Geotherm. Res. 148, 234–252.

Hicks, P. D., Matthews, A. J., Cooker, M. J., 2009a. The thermal structure of a gas-permeable

lava dome and time-scale separation in its response to perturbation. J. Geophys. Res. 122, doi: 10.1029/2008JB006198, published online.

Hicks, P. D., Matthews, A. J., Cooker, M. J., 2009b. Controls on the rate of rainfall infiltration into a volcanic lava dome. Geophys. Res. Lett., submitted.

Hort, M., Seyfried, R., Vöge, M., 2003. Radar Doppler velocimetry of volcanic eruptions: theoretical considerations and quantitative documentation of changes in eruptive behaviour at Stromboli volcano, Italy. Geophys. J. Int. 154, 515–532.

Jaquet, O., Carniel, R., Sparks, S., Thompson, G., Namar, R., Di Cecca, M., 2006. DEVIN: A forecasting approach using stochastic methods applied to the Soufrière Hills Volcano. J. Volcanol. Geotherm. Res. 153, 97–111.

Livezey, R. E., Chen, W. Y., 1983. Statistical field significance and its determination by Monte Carlo techniques. Mon. Wea. Rev. 111, 46–59.

Loughlin, S. C., Luckett, R., Christopher, T., Jones, L., Ryan, G., Strutt, M., Druitt, T., Baptie, B., 2009. Unprecedented gas release from a rapid, large volume dome collapse at Soufrière Hills Volcano, Montserrat, 20 May 2006. J. Volcanol. Geotherm. Res. 1, submitted.

Luckett, R., Baptie, B., Neuberg, J., 2002. The relationship between degassing and rockfall signals at Soufrière Hills Volcano, Montserrat. In Druitt, T.H., Kokelaar, B.P., (eds), 2002: The eruption of Soufrière Hills Volcano, Montserrat, from 1995 to 1999. Geological Society, London, Memoirs. 595–602.

Mason, B. G., Pyle, D. M., Dade, W. B., Jupp, T., 2004. Seasonality of volcanic eruptions. J. Geophys. Res. 109, B04206. doi: 10.1029/2002JB002293.

Mastin, L., 1994. Explosive tephra emissions at Mount St. Helens, 1989–1991 — The violent escape of magmatic gas following storms. Geol. Soc. Amer. Bull. 106, 175–185.

Matthews, A. J., Barclay, J., 2004. A thermodynamical model for rainfall-triggered volcanic dome collapse. Geophys. Res. Lett. 31, L05614. doi: 10.1029/2003GL019310.

Matthews, A. J., Barclay, J., Carn, S., Thompson, G., Alexander, J., Herd, R., Williams, C., 2002. Rainfall-induced volcanic activity on Montserrat. Geophys. Res. Lett. 29, 1644. doi: 10.1029/2002GL014863.

Miller, A. D., Stewart, R. C., White, R. A., Luckett, R., Baptie, B. J., Aspinall, W. P., Latchman, J. L., Lynch, L. L., Voight, B., 1998. Seismicity associated with dome growth and collapse at the Soufrière Hills Volcano, Montserrat. Geophys. Res. Lett. 25, 3401–3404.

Neuberg, J., 2000. External modulation of volcanic activity. Geophys. J. Int. 142, 232–240.

Neuberg, J., Baptie, B., Luckett, R., Stewart, R., 1998. Results from the broadband seismic network on Montserrat. Geophys. Res. Lett. 25, 3661–3664.

Neuberg, J., Luckett, R., Baptie, B., Olsen, K., 2000. Models of tremor and low-frequency earthquakes swarms on Montserrat. J. Volcanol. Geotherm. Res. 101, 83–104.

Neuberg, J., Tuffen, H., Collier, L., Green, D., Powell, T., Dingwell, D., 2006. The trigger mechanism of low-frequency earthquakes on Montserrat. J. Volcanol. Geotherm. Res. 153, 37–50.

Norton, G. E., Watts, R. B., Voight, B., Mattioli, G. S., Herd, R. A., Young, S. R., Devine, J. D., Aspinall, W. P., Bonadonna, C., Baptie, B. J., Edmonds, M., Harford, C. L., Joly, A. D., Loughline, S. C., Lucket, R., Sparks, R. S. J., 2002. Pyroclastic flow and explosive activity at Soufrière Hills

Volcano, Montserrat, during a period of virtually no magma extrusion. In Druitt, T.H., Kokelaar, B.P., (eds), 2002: The eruption of Soufrière Hills Volcano, Montserrat, from 1995 to 1999. Geological Society, London, Memoirs. 467–481.

Robertson, R., Cole, P., Sparks, R. S. J., Harford, C., Lejeune, A. M., McGuire, W. J., Miller, A. D., Murphy, M. D., Norton, G., Stevens, N. F., Young, S. R., 1998. The explosive eruption of Soufrière Hills Volcano, Montserrat, West Indies, September 17, 1996. Geophys. Res. Lett. 25, 3429–3432.

Roman, D. C., Neuberg, J., Luckett, R. R., 2006. Assessing the likelihood of volcanic eruption through analysis of volcanotectonic earthquake fault-plane solutions. Earth Planet. Sci. Lett. 248, 244–252.

Rowe, C. A., Thurber, C. H., White, R. A., 2004. Dome growth behavior at Soufrière Hills Volcano, Montserrat, revealed by relocation of volcanic event swarms, 1995–1996. J. Volcanol. Geotherm. Res. 134, 199–221.

Simmons, J., Elsworth, D., Voight, B., 2004. Instability of exogenous lava lobes during intense rainfall. Bull. Volcanol. 66, 725–734.

Taron, J., Elsworth, D., Thompson, G., Voight, B., 2007. Mechanisms for rainfall-concurrent lava dome collapses at Soufrière Hills Volcano, 2000–2002. J. Volcanol. Geotherm. Res. 160, 195–209.

Violette, S., de Marsily, G., Carbonnel, J. P., Goblet, P., Ledoux, E., Tijani, S. M., Vouille, G., 2001. Can rainfall trigger volcanic eruptions? A mechanical stress model of an active volcano: "Piton de la Fournaise", Reunion Island. Terra Nova 13, 18–24.

Yamasato, H., Kitagawa, S., Komiya, M., 1998. Effect of rainfall on dacitic lava dome collapse at Unzen volcano, Japan. Pap. Meteorol. Geophys. 48, 73–78.

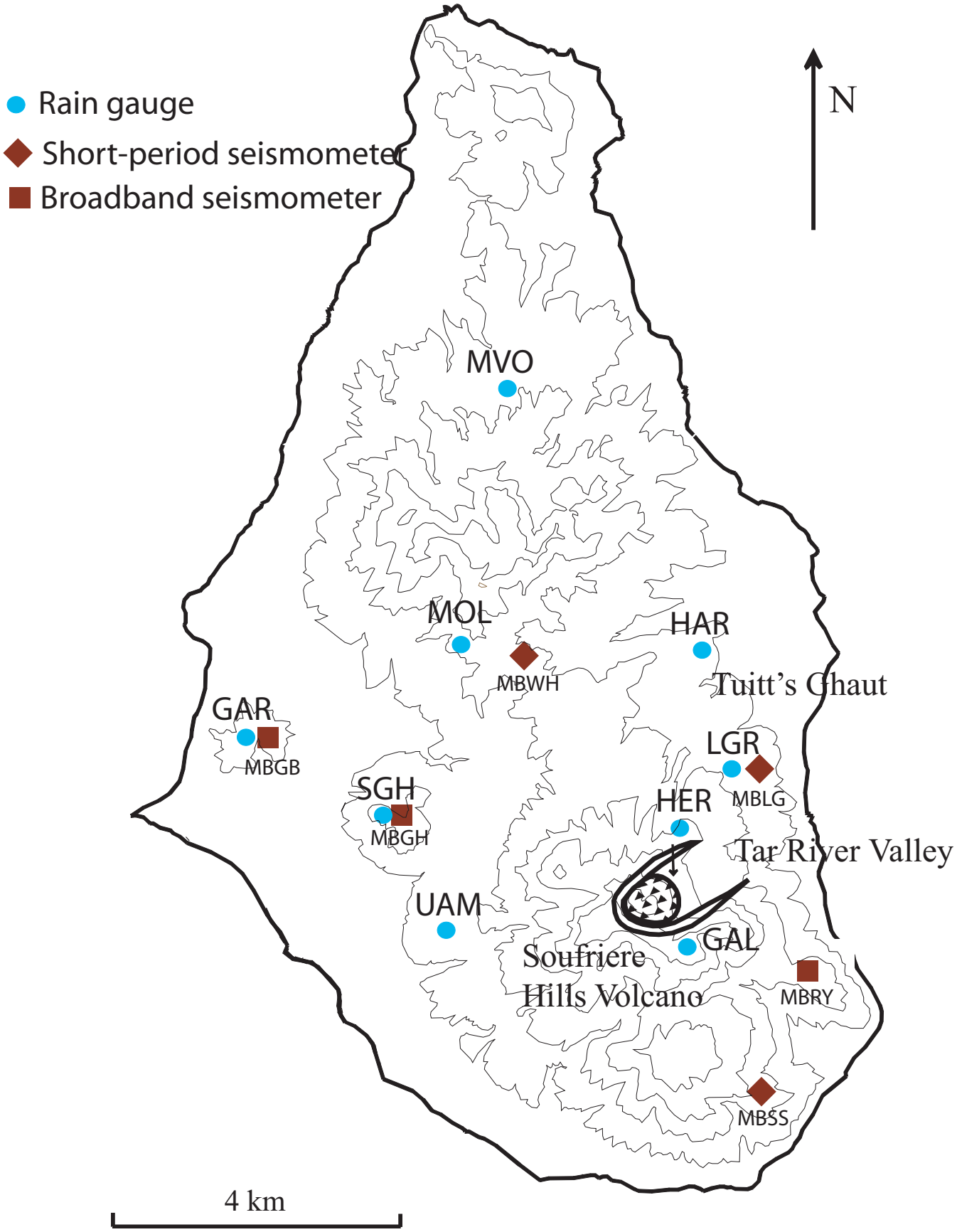

Figure 1: Map of Montserrat, showing the location of the Soufrière Hills Volcano, and the rain gauges (MVO, MVO North; MOL, Molyneux; GAR, Garibaldi Hill; SGH, St. George's Hill; HAR, Harris; LGR, Long Ground; HER, Hermitage; UAM, Upper Amersham; GAL, Galways), short-period seismometers (MBWH, Windy Hill; MBLG, Long Ground; MBSS, South Soufrière Hills) and broadband seismometers (MBGB, Garibaldi Hill; MBGH, St. George's Hill; MBRY, Roche's Yard).

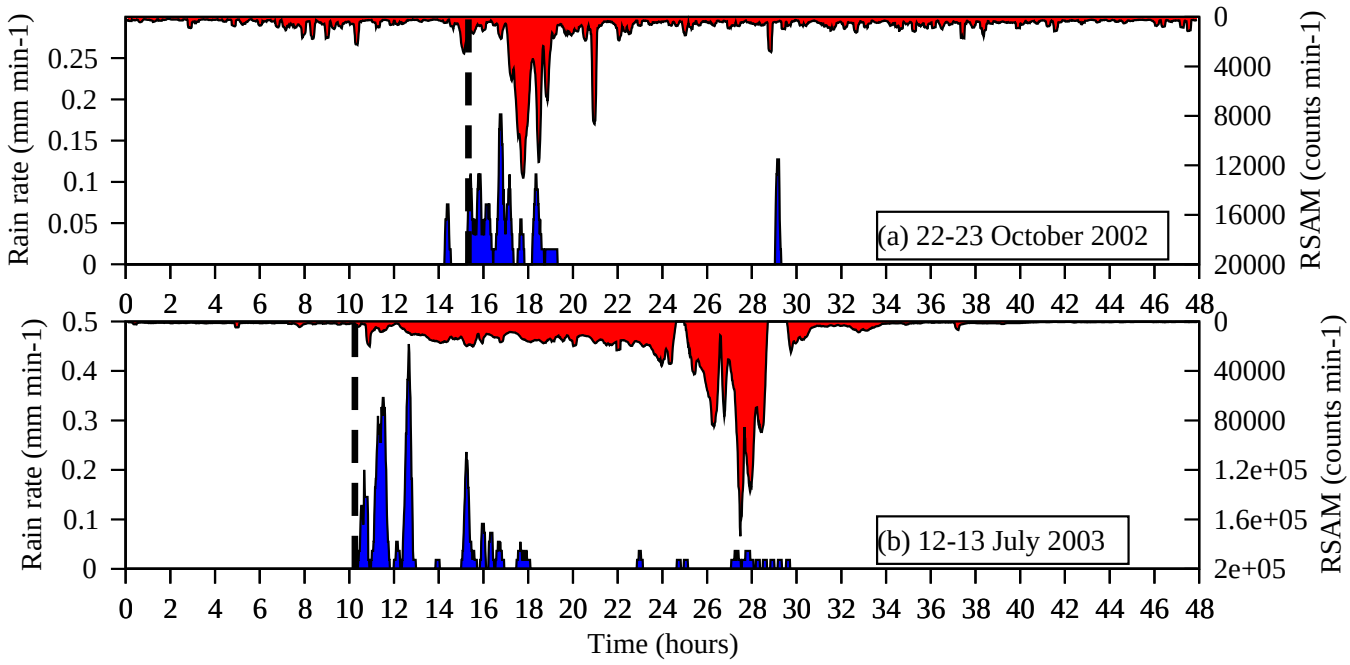

Figure 2: Time series of 10-minute averaged rainfall rate (lower data and left axis) and RSAM from Long Ground (upper data and right axis, inverted) for 48-hour periods starting at (a) 00 UTC 22 October 2002: precipitation from MVO North, (b) 00 UTC 12 July 2003: precipitation from Garibaldi Hill. The timing of the rainfall events, as defined in section 2.1, are indicated by the thick dashed vertical lines.

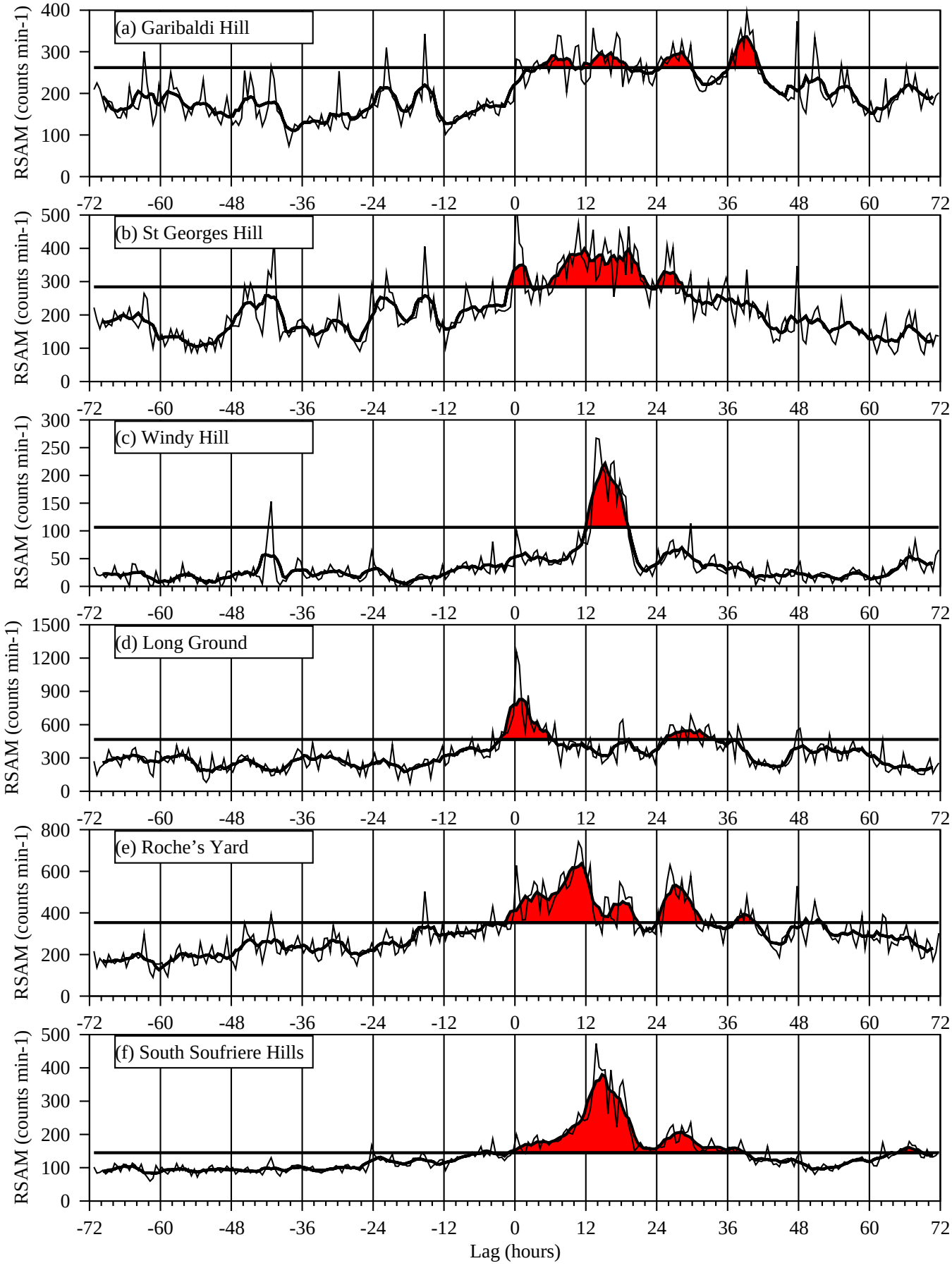

Figure 3: Composite RSAM anomalies, lagged relative to the start of rainfall events, for (a) Garibaldi Hill, (b) St George's Hill, (c) Windy Hill, (d) Long Ground, (e) Roche's Yard, (f) South Soufrière Hills. A rainfall threshold of 5 mm in 1 hr was used, with a 24 hr repose period. The thick line shows a 7-point running mean, and the horizontal line shows the 95% local significance level of this running mean from a Monte Carlo simulation. Values above the 95% local significance level are shaded.

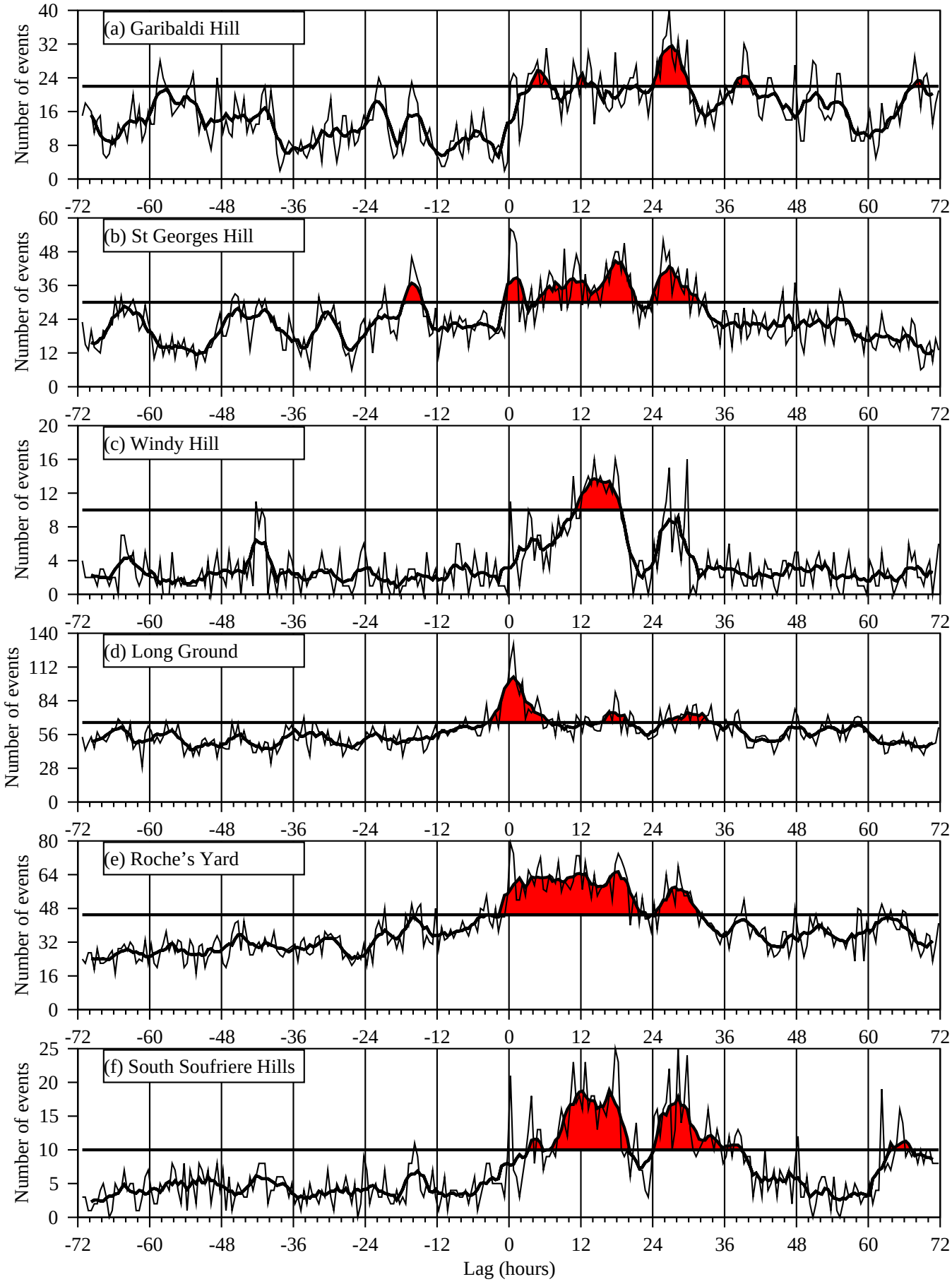

Figure 4: As Fig. 3 but for number of seismic events above a seismic threshold of 500 counts min^{-1}.

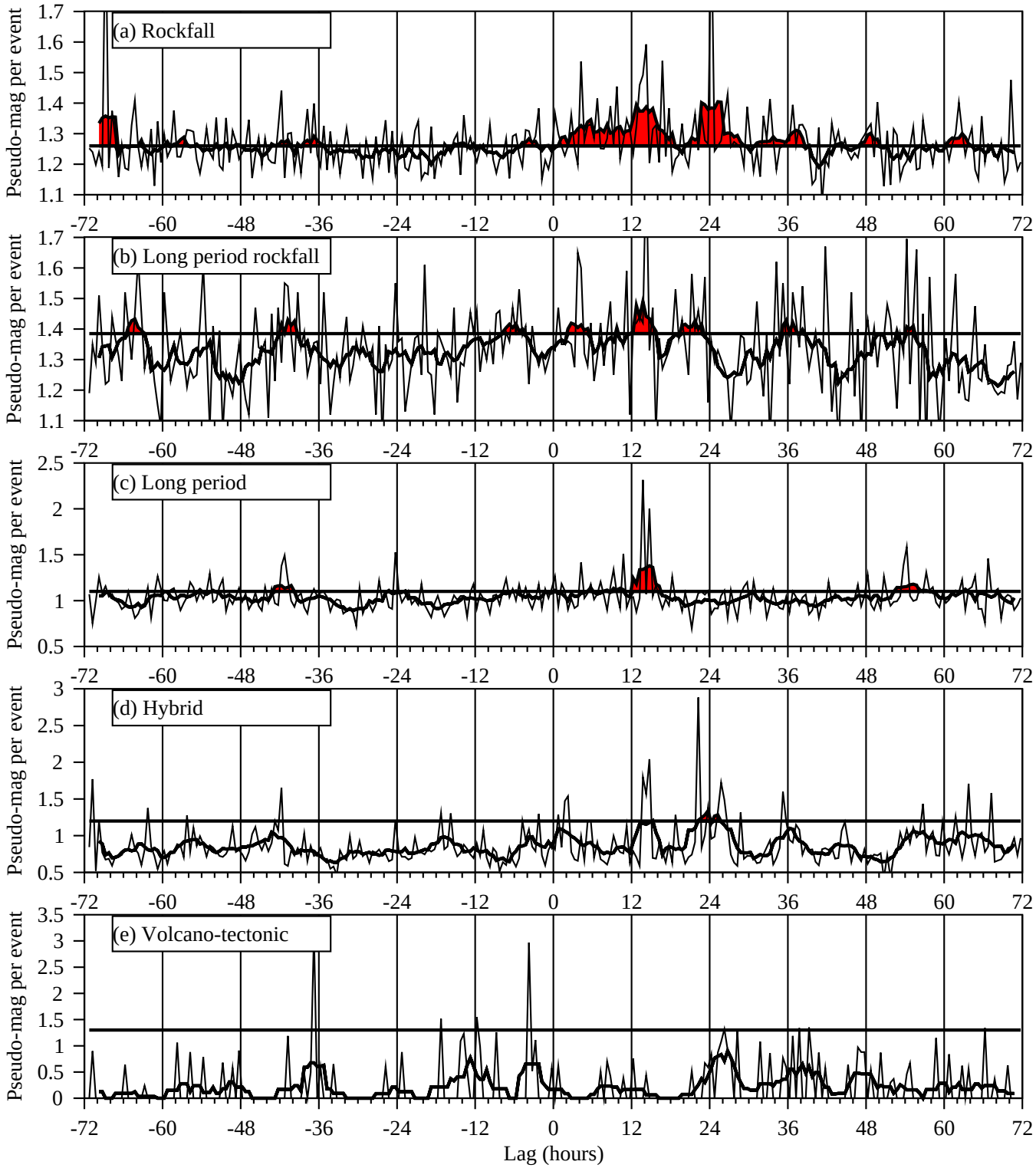

Figure 5: Composite of pseudo-magnitude of classified events, lagged relative to the start of rainfall events, for (a) rockfall, (b) long-period rockfall, (c) long-period (d) hybrid, (e) volcano–tectonic events. A rainfall threshold of 5 mm in 1 hr was used, with a 24 hr repose period. The thick line shows a 7-point running mean, and the horizontal line shows the 95% significance level of this running mean from a Monte Carlo simulation. Values above the 95% significance level are shaded.

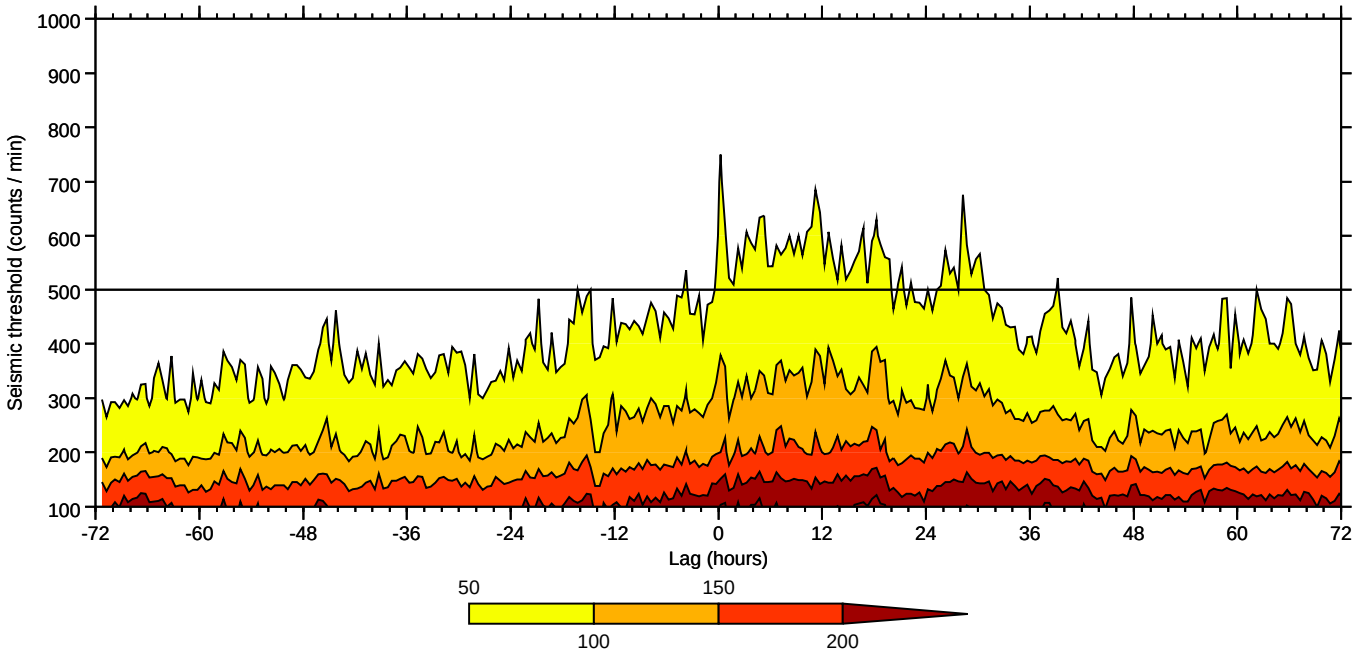

Figure 6: Composite of number of seismic events at Roche's Yard, as a function of lag relative to the start of rainfall events, and seismic threshold. Contour interval is 50 counts min^{-1}. Shading is shown by the legend. A rainfall threshold of 5 mm in 1 hr was used, with a 24 hr repose period. The composite in Fig. 4e is a cross-section through this figure, at the standard threshold level of 500 counts min^{-1}, indicated by the horizontal line.

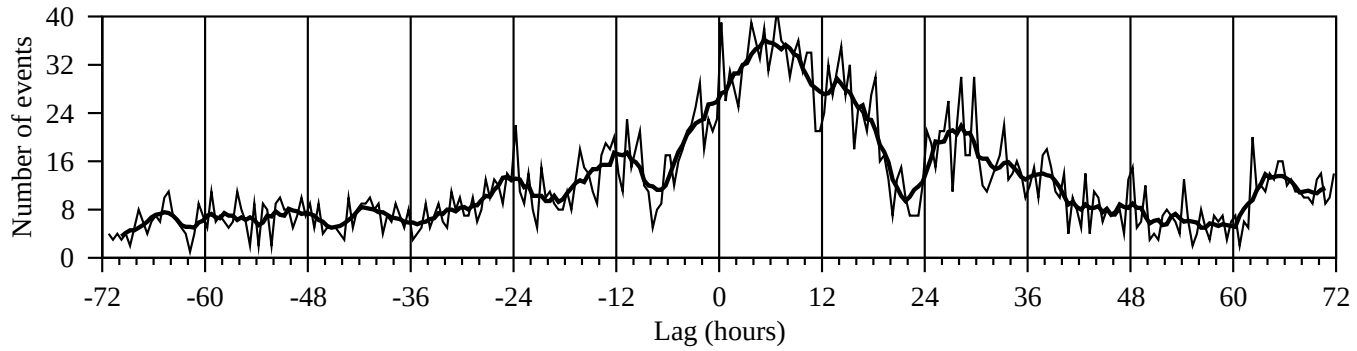

Figure 7: As Fig. 4 but for South Soufrière Hills seismometer only, with a repose period of 1 hour.

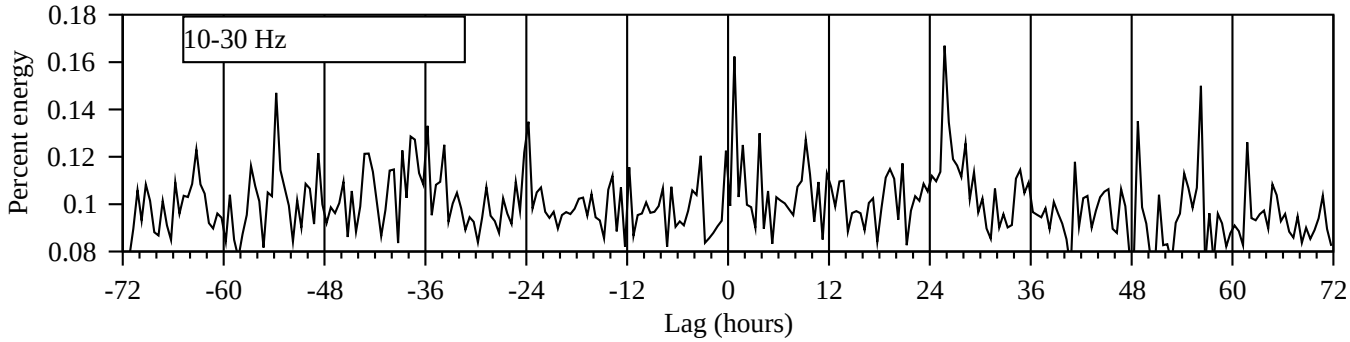

Figure 8: Composite of percentage energy per event in the 10–30 Hz frequency band, lagged relative to the start of rainfall events. A rainfall threshold of 5 mm in 1 hr was used, with a 24 hr repose period.

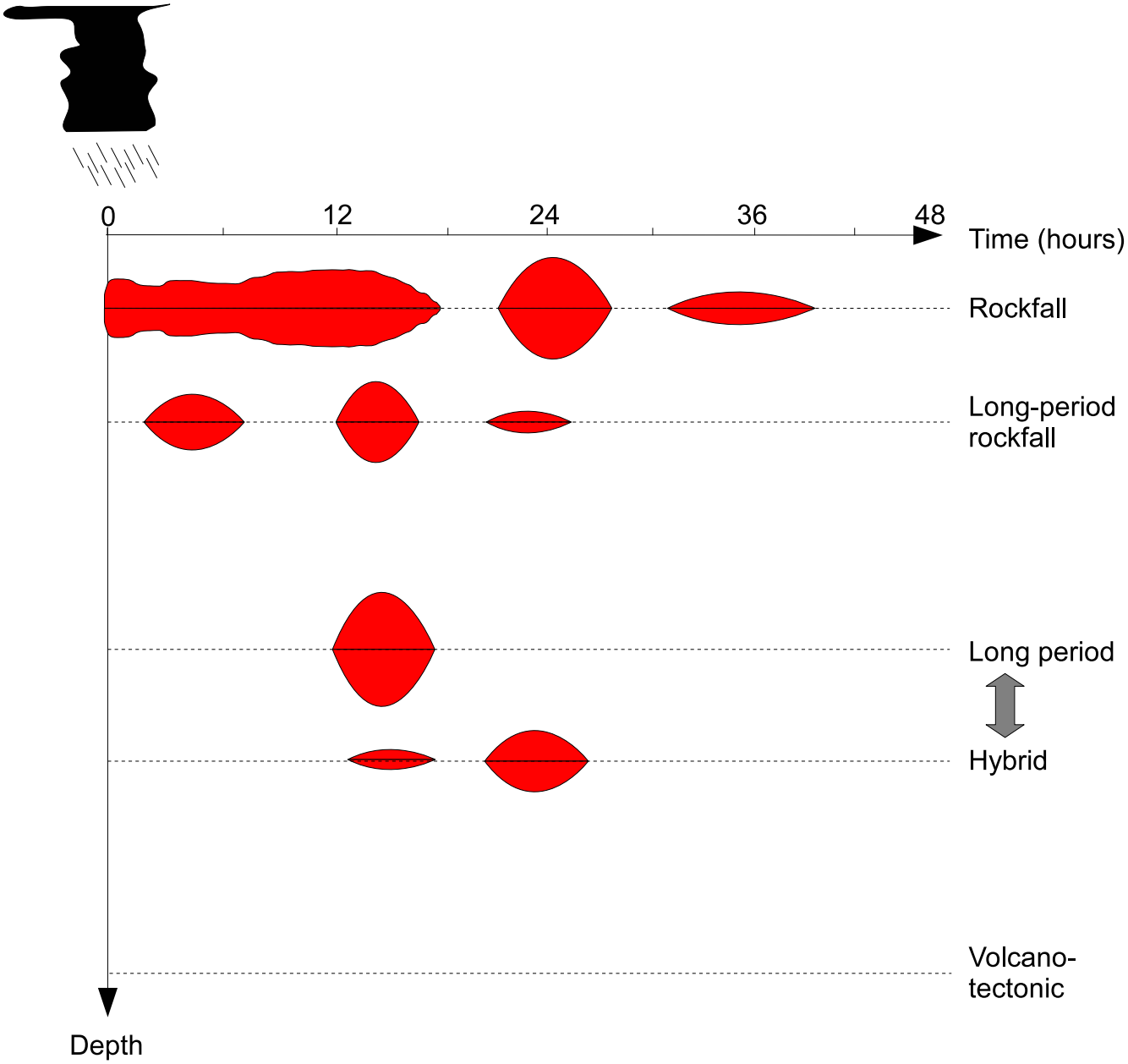

Figure 9: Schematic of observed volcano-seismic responses to rainfall, as a function of time after start of rainfall events and depth into the volcanic system.